J Mater Sci (2007) 42:10052–10057
DOI 10.1007/s10853-007-2051-6

Mn-doping effect on dielectric and electromechanical losses in the system $Pb(Zr_xTi_{1-x})O_3$–$Pb(Zn_{1/3}Nb_{2/3})O_3$

Rashed A. Islam · Shashank Priya · Ahmed Amin

Received: 8 October 2006 / Accepted: 9 July 2007 / Published online: 21 August 2007

Absract Dielectric and electromechanical losses play a critical role in the performance of the transducer in high power conditions. In this study, we report a systematic study on the effect of Mn-doping on the losses in the $Pb(Zr_xTi_{1-x})O_3$–$Pb(Zn_{1/3}Nb_{2/3})O_3$ (PZT–PZN) system. Two types of sintering conditions were employed to synthesize ceramics with varying grain sizes. The Zr/Ti ratio in the PZT system was fixed at 52/48 corresponding to morphotropic phase boundary (MPB) and Mn concentration was varied from 0 to 0.9 wt%. The results show that the composition 0.9PZT–0.1PZN + 0.5 wt% Mn provides optimized magnitude for the dielectric, piezoelectric, and loss properties.

Introduction

In sonar transducers, a high acoustical damping is required in order to have broad band electromechanical properties. To achieve high acoustical damping, generally transducers are designed with as low a Q_A ($1/Q_A$ is the damping done by the load ($1/Q_A = 1/Q_m - 1/Q$), Q is mechanical quality factor of the piezoceramic under zero load and Q_m is the mechanical quality factor under an external load) as possible. However, this presents a limiting problem for applications in projectors, as even low dielectric losses in the presence of large AC electrical driving fields becomes important in limiting the far-field acoustical source projection. In these transducer designs, high values of Q are required for optimum transducer performance. For a piezoelectric material suitable for projectors it is essential that it satisfies the requirement of high power actuator and transducer. This implies that the material should have large electromechanical coupling factor (k), Q_m, and piezoelectric constant (d). Further a high dielectric constant (ε) is required in order to draw large power with low dielectric loss. Consequently, designing a high power material for projectors involves generation of "hard" and "soft" properties at the same time [1–3]. This presents a limiting problem for materials design, as high piezoelectric constants and electromechanical constants are usually accompanied by higher dielectric losses [1]. Figure 1 shows the general strategy adopted in order to achieve this combination of properties. Generally, PZT is modified with a complex A or B-site ion (Pb-based relaxor type materials) in various ratios and some acceptor ion is added to this composition. Adding the relaxor type compounds enhances the piezoelectric properties of the material while the acceptor ion increases the mechanical quality factor and reduces dielectric losses.

One of the important parameter for the selection of the material for high power application is the magnitude of the electro transduction power generated. The power radiated in a medium with specific acoustic impedance Z_a is given as [4]:

$$P = 4\pi^2 \mathrm{Re}(Z_a) A^2 f^2 u^2 \quad (1)$$

where $\mathrm{Re}(Z_a)$ is the real part of Z_a, A is the radiating area, u is the rms mechanical displacement, and f is the frequency. For high power high frequency resonance application, power radiated is limited by the vibration velocity (v_o)

R. A. Islam · S. Priya (✉)
Materials Science and Engineering, Automation & Robotics Research Institute, The University of Texas, Arlington, TX 76019, USA
e-mail: spriya@uta.edu

A. Amin
Naval Undersea Warfare Center, Newport, RI, USA

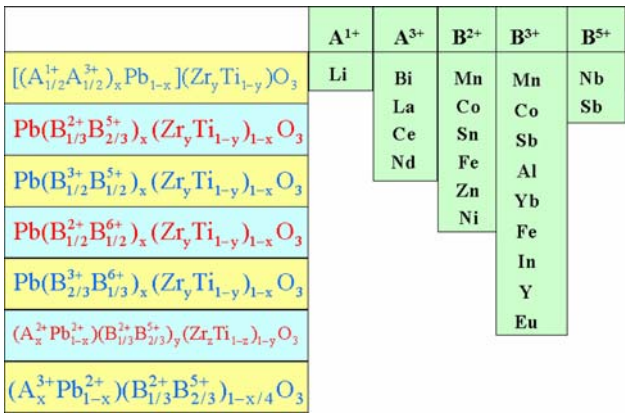

Fig. 1 Possible compositional variations in order to achieve the combinatory hard and soft characteristics in the PZT ceramics

given as $\upsilon_o = 2\,\pi f\, u$ and mechanical quality factor (Q_m). At resonance, for a low Q_m material, the mechanical displacement is low (approximately for bar poled along 3 direction), $u = (8/\pi^2)Q_m d_{31} E_3 L$ [5], so the dielectric losses will be the limiting case, while for a high Q_m material, u will be high so mechanical losses are the limiting factor. The dissipated power per unit volume due to the dielectric losses is given by [6]:

$$P_D = \omega E_3^2 \varepsilon_o \varepsilon_{33}^T \tan\delta \tag{2}$$

Heat generation at the resonance is caused by the dissipated-vibration-energy ($\varpi_o U$), which can be represented in terms of the vibration velocity (υ_o) and several material constants, given as [7, 8]:

$$\varpi_o U = \frac{1}{2} M \upsilon_0^2 \varpi_o Q_m^{-1} = \frac{1}{4} Y x_m V \varpi_o Q_m^{-1} = \xi \varpi_o Q_m^{-1} \tag{3}$$

where ϖ_o is the resonant angular frequency, M, Y, and V are the mass, Young's modulus and volume of the material, x_m is the maximum strain, and ξ is the stored elastic energy in the material. The temperature rise (θ) in the material due to dielectric losses can be approximated by taking into account only the convection heat transfer (h = 10 W m^{-2} K^{-1} for free air) [1]:

$$\theta = P_D t / 2h \tag{4}$$

Hence, at resonance the temperature rise is governed by dielectric and mechanical loss as given by Eqs 3 and 4 and both are dependent upon the electric field. In the off-resonance condition the temperature rise is governed by dielectric loss. It should be noted here that the two losses are related to each other through piezoelectric and elastic constants and the change in the magnitude of one affects the magnitude of other [9]. The performance of a piezoelectric transducer has previously been estimated as given in Eq. (5); where η is the electromechanical efficiency [4],

$$\eta = \frac{1 - Q_m/Q}{1 + \frac{1}{k^2}\frac{\tan\delta}{Q_m}} \approx 1 - Q_A \frac{1}{Q} - \frac{1}{k^2}\frac{1}{Q_A}\tan\delta \tag{5}$$

where k is the effective electromechanical coupling coefficient of the transducer. Thus, a larger dielectric loss will result in the reduction of the transducer efficiency considerably.

Losses are known to increase with the applied temperature and pressure causing further degradation in the transducer performance. Figure 2 shows the variation of the dielectric loss factor as a function of the uniaxial compressive stress at room temperature (20 °C) when the material was driven under AC field of 0.39 MV/m with a DC bias of 0.79 MV/m. The data is shown for base composition given as $0.9[Pb(Zr_{0.61},Ti_{0.39})O_3]-0.1[Pb(Mn_{1/3}Nb_{2/3})O_3]$ (Composition #1)and its modification with 0.2, 0.5, and 1 ml% Yb_2O_3 (Composition 2, 3, and 4). Clearly, the data shows that under high field–high pressure drive the loss factor reaches a high magnitude of 8–12%. Figure 3 shows the dielectric loss factor data for the commercial APC 841 ceramics as a function of temperature. The data was measured under high field conditions (0.39 MV/m with a DC bias of 0.79 MV/m) with a constant uniaxial pressure of 42 MPa. Again, the loss factor magnitude reaches the values of 7–11%. These numbers reflect that the important strategy in the design of the high performance transducer is reduction of the dielectric loss factor.

The objective of this manuscript is to optimize the magnitude of the dielectric loss factor and mechanical quality factor in the Mn modified $0.9Pb(Zr_{0.52}Ti_{0.48})O_3$–$0.1Pb(Zn_{1/3}Nb_{2/3})O_3$ (PZT–PZN) system. Recently, this

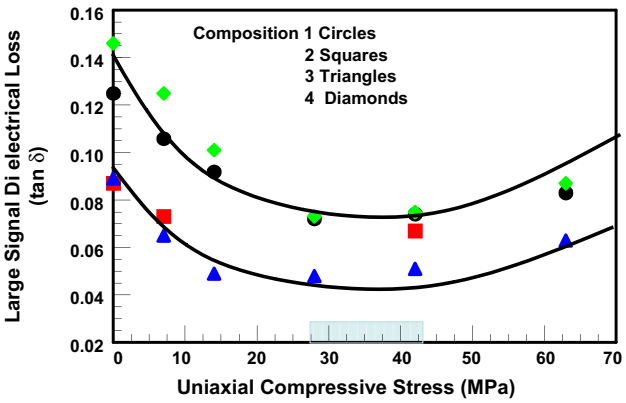

Fig. 2 Variation of the dielectric loss factor as a function of the uniaxial compressive stress at room temperature (20 °C) when the material was driven under AC field of 0.39 MV/m with a DC bias of 0.79 MV/m. Base composition is given as $0.9[Pb(Zr_{0.61}Ti_{0.39})O_3]$ $0.1[Pb(Mn_{1/3}Nb_{2/3})O_3]$ (Composition #1)and its modification with 0.2, 0.5, and 1 ml% Yb_2O_3 as composition 2, 3, and 4

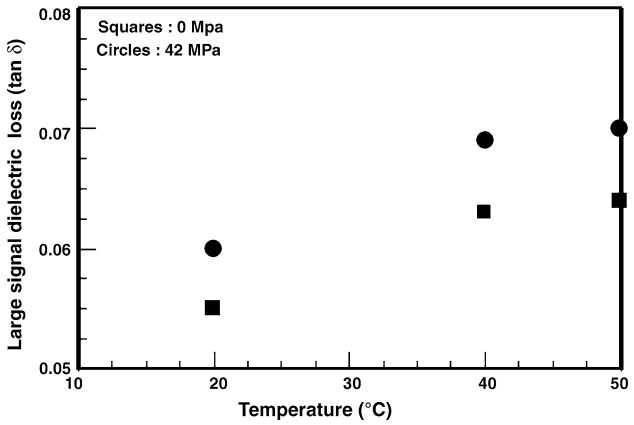

Fig. 3 Dielectric loss factor data for the commercial APC 841 ceramics as a function of temperature under high field drive

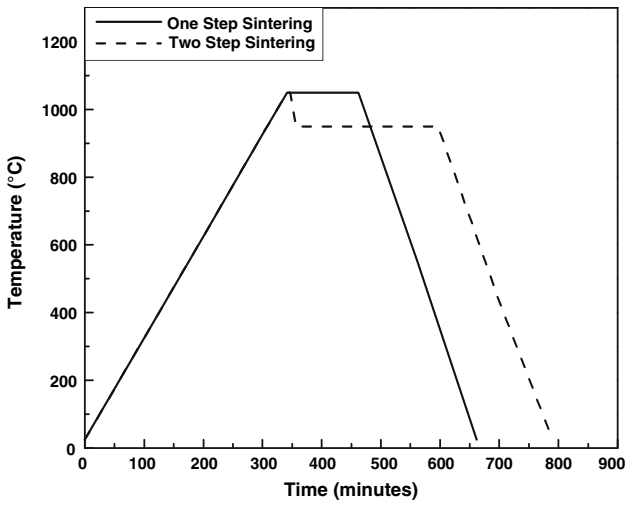

Fig. 4 Schematic illustration of single-step and two-step sintering profiles

system has been shown to be promising for the high power applications [3]. The optimization was conducted with respect to sintering temperature profile and Mn concentration. All the results are reported at room temperature and atmospheric pressure.

Experimental procedure

Reagent-grade powders of PbO, ZrO_2, ZnO, Nb_2O_5, $MnCO_3$, and TiO_2 were obtained from Alfa Aesar, Co. MA. USA. Stoichiometric ratios of the powders corresponding to composition of $0.9Pb(Zr_{0.52}Ti_{0.48})O_3$–$0.1Pb(Zn_{1/3}Nb_{2/3})O_3$ + y wt% $MnCO_3$ (y = 0, 0.5, 0.7, 0.9) were ball-milled with ethyl alcohol and YSZ grinding media (5 mm diameter, Tosoh Co. Tokyo, Japan) in a polyethylene jar for 24 h. After drying, the 0.9 PZT (52:48)−0.1PZN + y wt% $MnCO_3$ powders were calcined at 750 °C for 2 h. Calcined powders were crushed, sieved using US mesh # 270 and then ball milled separately with alcohol and grinding media for 24 h. After ball milling the powders were dried at 80 °C and sieved in a stainless steel sieve of US mesh #170. Sieved powders were pressed to pellets of size 12.7 × 1.5 mm^2 in a hardened steel die using a hydraulic press under pressure of 15 MPa. The green body was cold isostatically pressed at 207 MPa. After CIP the samples were sintered in air atmosphere using Thermolene 6000 furnace in the temperature range of 950–1,100 °C for 2 h (for single-step sintering profile). Other samples were placed in a Lindberg BlueM furnace for two-step sintering. In this profile the samples were kept at a high temperature for 5 min (1,050, 1,000, and 950 °C) and then cooled rapidly to a lower temperature (950, 925, and 900 °C respectively) and held for 4 h. Figure 4 shows the illustration of single-step and two-step sintering profiles. It is well known that the grain size increases with sintering temperature. Thus, two-step sintering provides a method for obtaining dense ceramics with lower grain sizes [10]. Figure 5 shows the variation in the grain size with the sintering temperature for two-step profile clearly showing that lower grain sizes are obtained with reducing sintering temperatures.

The density of samples was measured by Archimedes principle. X-ray diffraction analysis was performed using Siemens Krystalloflex 810 D500 X-ray diffractometer on samples after each step of calcination and sintering. Microstructural analysis of the sintered samples was done using Zeiss Leo Smart SEM on the polished and thermally etched samples. The average grain size was determined from SEM micrograph using linear intercept method. In

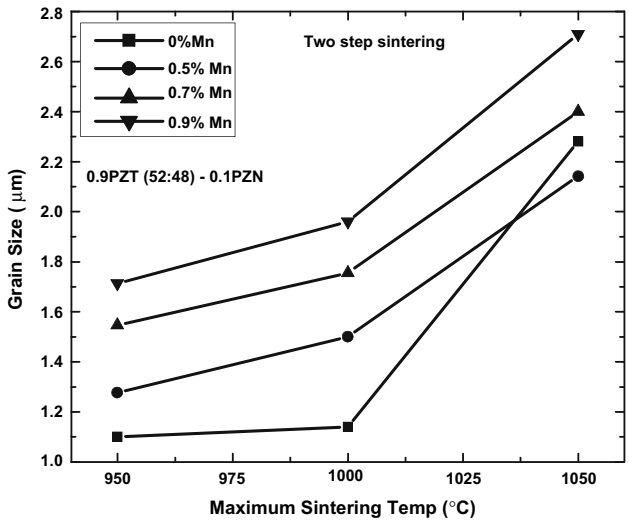

Fig. 5 Variation in the grain size with the sintering temperature for two-step profile

order to perform the piezoelectric measurements, Ag/Pd electrode was applied on the samples and fired at 850 °C for 1 h. The electroded specimens were poled by applying a DC field of 3–4 kV/mm for 20–30 min in a silicone oil bath at 80–120 °C. Two to four samples of each batch were poled for the piezoelectric measurement and the average value was recorded. The piezoelectric constant was measured by using APC YE 2730A d_{33} meter (±1%). Resonance characteristics were determined using HP 4194A impedance analyzer (Hewlett Packard Co. USA). Dielectric constant as a function of temperature was measured using HP 4274A LCR meter (Hewlett Packard Co. USA, ±0.13%).

Results and discussion

Defects and substituents are known to affect the electromechanical properties of the normal ferroelectrics in both poled and unpoled conditions. Generally, acceptor doping in the PZT-based ceramics results in (i) decreased dielectric constant and loss, (ii) lower elastic compliance, (iii) lower electromechanical coupling factor, and (iv) lower electromechanical losses. In acceptor modified materials, oxygen vacancies are created for charge compensation, which are frozen into the ceramic during quenching from high temperature. These oxygen vacancies can reside in the material in many possible ways: (i) associated defect dipole structure with acceptor (ii) diffuse to domain walls or (iii) compensate the local charge fluctuation at domain walls [1, 11]. The mechanism for introduction of "hard" properties depends on the way in which oxygen vacancies distribute themselves. In Mn-modified PZT ceramics, it is believed that hardening occurs due to the pinning of domain boundaries by Mn-oxygen vacancy defect structure. Further, it is believed that Mn^{+3} attaches strongly to oxygen vacancies due to Jahn Teller effect. This prevents conduction and reduces the domain wall mobility resulting in reduced losses.

Figure 6a shows the variation of the radial mode coupling factor (k_p) as a function of the sintering temperature for one step profile. The variation of k_p with sintering temperature was similar for all the compositions, increasing in the range of 950–1,050 °C and decreasing at higher sintering temperature. A k_p of greater than 0.6 was obtained for the composition with 0.5 wt% Mn in the sintering range of 950–1,050 °C. Figure 6b shows the variation of k_p with maximum sintering temperature in two-step profile. Again, a high k_p of 0.6 was obtained for the composition with 0.5 wt% Mn. The grain size has strong effect on the magnitude of the dielectric and piezoelectric properties. As the grains become finer, under the same electric field, the absolute value of the strain decreases and the hysteresis becomes smaller [11]. This is explained by the increase in

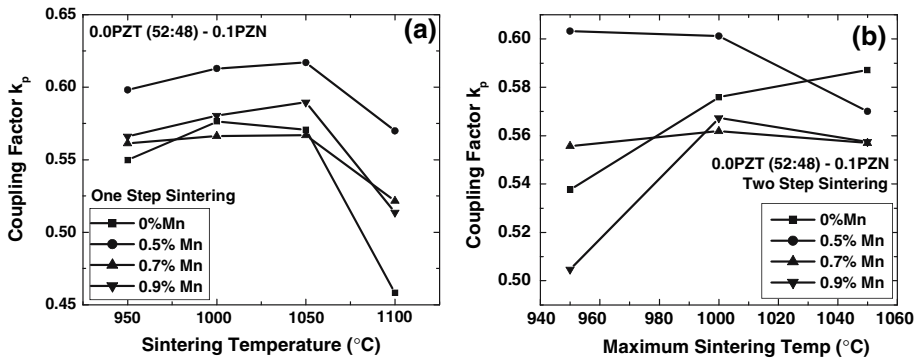

Fig. 6 Variation of the radial mode coupling factor (k_p) as a function of the sintering temperature (**a**) one-step profile, and (**b**) two-step profile

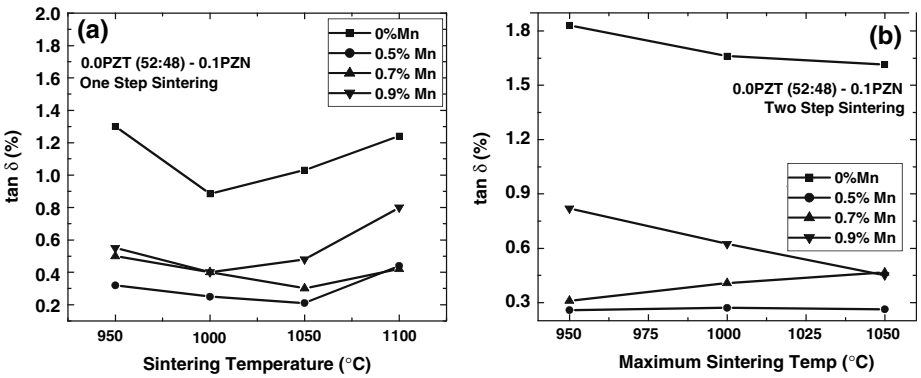

Fig. 7 Variation of the dielectric loss factor (tanδ) as a function of the sintering temperature (**a**) one-step profile, and (**b**) two-step profile

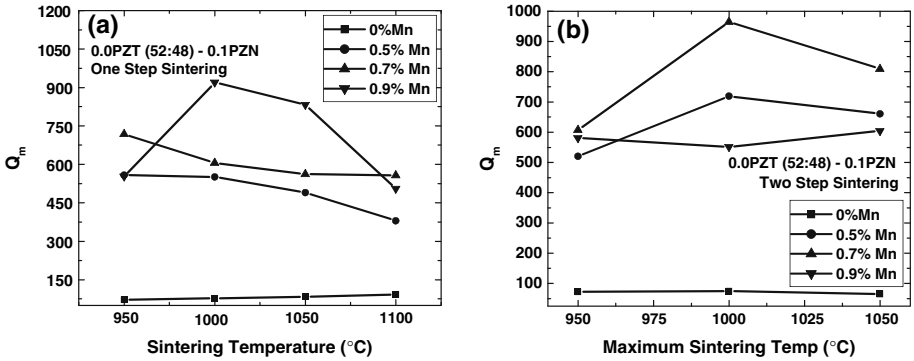

Fig. 8 Variation of the mechanical quality factor (Q_m) as a function of the sintering temperature (**a**) one-step profile, and (**b**) two-step profile

Table 1 List of the piezoelectric and dielectric properties for all the compositions synthesized in this study with different sintering conditions

Composition	Sintering profile	Sintering temperature	d_{33} (pC/N)	ε_r
0.9 $Pb(Zr_{0.52}Ti_{0.48})O_3$ − 0.1 $Pb(Zn_{1/3}Nb_{2/3})O_3$ + 0 (wt%) $MnCO_3$	One-step	950 °C	370	1,914
		1,000 °C	435	2,132
		1,050 °C	445	2,025
		1,100 °C	371	1,736
	Two-step	950–900 °C	390	1,588
		1,000–925 °C	429	1,798
		1,050–950 °C	442	1,981
0.9 $Pb(Zr_{0.52}Ti_{0.48})O_3$ − 0.1 $Pb(Zn_{1/3}Nb_{2/3})O_3$ + 0.5 (wt%) $MnCO_3$	One-step	950 °C	415	1,551
		1,000 °C	431	1,600
		1,050 °C	457	1,688
		1,100 °C	389	1,665
	Two-step	950–900 °C	317	1,221
		1,000–925 °C	372	1,173
		1,050–950 °C	340	1,160
0.9 $Pb(Zr_{0.52}Ti_{0.48})O_3$ − 0.1 $Pb(Zn_{1/3}Nb_{2/3})O_3$ + 0.7 (wt%) $MnCO_3$	One-step	950 °C	330	866
		1,000 °C	305	763
		1,050 °C	290	752
		1,100 °C	280	719
	Two-step	950–900 °C	272	613
		1,000–925 °C	291	594
		1,050–950 °C	285	608
0.9 $Pb(Zr_{0.52}Ti_{0.48})O_3$ − 0.1 $Pb(Zn_{1/3}Nb_{2/3})O_3$ + 0.9 (wt%) $MnCO_3$	One-step	950 °C	310	808
		1,000 °C	300	755
		1,050 °C	290	735
		1,100 °C	282	699
	Two-step	950–900 °C	255	685
		1,000–925 °C	270	689
		1,050–950 °C	265	684

coercive field for 90° domain rotation with decreasing grain size. With decreasing grain size, ferroelectric domain walls become difficult to form in the grain, and the domain rotation contribution to the strain becomes smaller. Thus, for the Mn-modified PZT–PZN it can be expected that the coupling factor increases with the Mn concentration as there is pronounced increase in the grain size (Fig. 5) for compositions given by 0.9PZT–0.1PZN + y wt% Mn. On the other hand, dielectric and piezoelectric decrease with the acceptor modification due to hardening effect. Thus, the data in Fig. 6b is the average of the changes in piezoelectric and dielectric properties occurring due to acceptor

modification and grain size increase, both being complementary to each other.

Figure 7a shows the dielectric loss factor data as a function of the sintering temperature in one-step profile. The composition with 0.5 wt% Mn exhibited the lowest loss factor over the whole temperature range. The loss factor magnitude was lowest at the sintering temperature of 1,050 °C having magnitude of 0.2% (and highest k_p of 0.61). Figure 7b shows the variation of loss factor as a function of maximum sintering temperature in two-step profile. Again the composition with 0.5 wt% Mn exhibited the lowest loss factor with the magnitude of 0.27%. Figure 8a shows the variation of Q_m as a function of the sintering temperature in one-step profile. A significant increase in the Q_m is obtained with Mn modification indicating the induction of the hardening effect. The magnitude of the Q_m for the composition with 0.5 wt% Mn was 490 at sintering temperature of 1,050 °C and 551 at sintering temperature of 1,000 °C. Figure 8b shows the variation of Q_m as a function of maximum sintering temperature in two-step profile. The magnitude of the Q_m for the composition with 0.5 wt% Mn at sintering temperature of 1,000 °C was 719 ($\tan\delta = 0.27$ and $k_p = 0.61$). Thus, combining the results of Figs. 7 and 8 it can be hypothesized that 0.9PZT–0.1PZN + 0.5 wt% Mn represents optimized composition.

Table 1 lists the piezoelectric and dielectric properties of all the compositions synthesized in this study. It is evident from this table that Mn induces hardening effect in the PZT–PZN ceramics as the magnitude of the dielectric and piezoelectric decreases with increasing Mn concentration. For the composition 0.9PZT–0.1PZN + 0.5 wt% Mn synthesized using one-step profile at 1,050 °C the magnitude of the d_{33} and ε_r was 457 pC/N and 1,688, respectively. Same composition synthesized using the two-step profile with maximum temperature of 1,000 °C had the magnitude of d_{33} and ε_r as 372 pC/N and 1,173. These magnitudes are promising for the high power application.

Conclusions

This manuscript reports the systematic study on the Mn-modified PZT–PZN system with variation in the synthesis condition. It was found that the composition 0.9PZT–0.1PZN + 0.5 wt% Mn provides optimized magnitude for the dielectric, piezoelectric, and loss properties. This composition synthesized using one-step profile with sintering temperature of 1,050 °C had the magnitude of coefficients as: $k_p = 0.61$, $\tan\delta = 0.2$, $Q_m = 490$, $d_{33} = 457$ pC/N, and $\varepsilon_r = 1{,}688$; while in two-step profile with maximum sintering temperature of 1,000 °C the magnitude of coefficients was: $k_p = 0.61$, $\tan\delta = 0.27$, $Q_m = 719$, $d_{33} = 372$ pC/N, and $\varepsilon_r = 1{,}173$.

References

1. Priya S (2003) PhD dissertation, Pennsylvania State University, University Park, PA
2. Chen Y-H, Uchino K, Viehland D (2001) J Appl Phys 89:3928
3. Priya S, Uchino K, Ryu J, Ahn C, Nahm S (2003) Appl Phys Lett 83:5020
4. Berlincourt D, Krueger H (1965) US Navy J Underwater Acoustics 15:266
5. Uchino K (1999) Piezoelectric actuators and ultrasonic motors. Kluwer Academic, Boston, MA
6. Chen W-H (1983) IEEE Trans Sonics Ultrasonics 30:238
7. Takahashi S, Sasaki Y, Hirose S, Uchino K (1995) Mater Res Soc Symp Proc 360:305
8. Takahashi S, Sasaki Y, Hirose S, Uchino K (1995) Jpn J Appl Phys 34:5328
9. Yamauchi F, Takahashi M (1970) J Phys Soc Jpn 28:313
10. Chen IW, Wang XH (2002) Nature 404(9):168
11. Uchino K (2000) Ferroelectric devices. Marcel Dekker Inc., New York, pp 57–69